International Journal of Mass Spectrometry 304 (2011) 41–44

Contents lists available at ScienceDirect

International Journal of Mass Spectrometry

journal homepage: www.elsevier.com/locate/ijms

Effect of isotopic content on the rate constants for the dissociative electron–ion recombination of N_2H^+

Patrick A. Lawson, David Osborne Jr., Nigel G. Adams*

Department of Chemistry, University of Georgia, Athens, GA 30602, USA

ARTICLE INFO

Article history:
Received 26 January 2011
Received in revised form 29 March 2011
Accepted 29 March 2011
Available online 8 April 2011

Keywords:
Isotopic reactions
Dissociative recombination
Flowing afterglow
Ion–electron recombination

ABSTRACT

The rate constants, α_e, for dissociative electron–ion recombination of various isotopic combinations of N_2H^+ have been determined at 300 and 500 K in a variable temperature flowing afterglow using a Langmuir probe to determine the electron density. The values of α_e at 300 K are 2.77 ($^{14}N_2H^+$), 2.12 ($^{14}N_2D^+$), 2.31 ($^{15}N_2H^+$) and 1.98 ($^{15}N_2D^+$) $\times 10^{-7}$ cm^3 s^{-1}. The equivalent values at 500 K are 2.84, 2.33, 2.93, and 2.33 respectively. This has shown that the greatest change occurs between H and D substitution $\alpha_e(^{14/15}N_2D^+)/\alpha_e(^{14/15}N_2H^+) \sim 0.765/0.857$ at 300 K and 0.820/0.795 at 500 K respectively. Values at 500 K are consistently larger than at 300 K. At both temperatures, the rate constants with H substitution are larger than with D substitution for both ^{14}N and ^{15}N. Values with ^{14}N substitution are larger than with ^{15}N for both H and D. At 500 K, the values are independent of whether the ion contains ^{14}N or ^{15}N. Gas-phase ^{15}N fractionation enhancement is predicted in many regions of the interstellar medium including cold and pre-stellar cores. The effect of this fractionation on the recombination process is investigated. The relevance to storage ring measurements of recombination rate constants is considered and applications to the chemistry of the interstellar medium are discussed.

1. Introduction

Due to nucleosynthesis, isotopic ratios are expected to vary in different parts of the galaxy and will provide information about the degree of nuclear processing in those regions. However, due to isotope fractionation in ion–molecule reactions and in electron–ion recombination, the fractionation observed in the molecules will differ from that in nuclearsynthetic processing. Such fractionation has been observed in several isotopes notably H/D [1], $^{14}N/^{15}N$ in N_2H^+ and NH_3 [2–6] and $^{12}C/^{13}C$ in CO [7]. Isotope fractionation has also been observed in CN and HCN in Comet 17P/Holmes [8] and in meteoritic and interplanetary dust [9]. H/D studies in N_2H^+ have been made for a series of prestellar cores by Crapsi et al. [10] and Fontani et al. [11] Because of the $^{15}N/^{14}N$ enhancement, a possible fractionation route such as:

$$H_3^+ + N_2 \rightarrow N_2H^+ + H_2 \quad (1)$$

$$^{14}N_2H^+ + {}^{14}N^{15}N \rightarrow {}^{14}N^{15}NH^+ + {}^{14}N_2 \quad (2)$$

was previously investigated in the laboratory [12]. These reactions were included in chemical models of the interstellar medium by Terzieva and Herbst [2] and by Rodgers and Charnley [3]. The latter authors also included the electron–ion recombination reactions.

$$^{14}N_2H^+ + e \rightarrow H + {}^{14}N_2 \quad (3)$$

and

$$^{14}N^{15}NH^+ + e \rightarrow H + {}^{14}N^{15}N \quad (4)$$

in their models. Following extensive studies, it has now been established that the only reaction channel in reaction (3) is that giving an N_2 molecule and an H atom [13] and, presumably, also in reaction (4) for other ^{14}N and ^{15}N combinations. The channel to NH + N was erroneously identified as dominant by Geppert et al. [14]. However, this was shown not to be the case (NH + N minor if at all) by Molek et al. [15], a result now also obtained by Geppert and Larsson [16]. Thus, reaction (2) enhances the observable ^{15}N in N_2H^+ and reaction (4) returns the ^{15}N to the neutral N_2. Thus, it is important to measure the specific recombination rate constants to be included in the models together with the fractionation reaction (2). Unfortunately, it is not readily possible to study reaction (4) in the flowing afterglow because of isotope fractionation reactions between $^{14}N_2$, $^{15}N_2$ and $^{14}N^{15}N$ forms of N_2 and N_2H^+. Therefore, only $^{14}N_2H^+$ and $^{15}N_2H^+$ recombination rate constants could be measured. However, this will give an indication of how the rate constants for dissociative recombination vary with isotopic substitution. In addition, for as complete a study as possible, the hydrogenated and deuterated forms of $^{14}N_2H^+$ and $^{15}N_2H^+$ recombination were also studied.

* Corresponding author. Tel.: +1 706 542 3722; fax: +1 706 542 9454.
E-mail address: ngadams@uga.edu (N.G. Adams).

1387-3806/$ – see front matter © 2011 Elsevier B.V. All rights reserved.
doi:10.1016/j.ijms.2011.03.013

Measurements were made at room temperature (300 K) and at 500 K to obtain some information on the temperature dependencies. However, more detailed studies could not be made because of the expenses of the reactant gases.

Also, detailed studies were not made at temperatures below 300 K because the association

$$N_2H^+ + N_2 + M \rightarrow H^+(N_2)_2 + M \quad (5)$$

(where M is the He carrier gas) can become competitive with recombination at lower temperatures due to the increasing association rate constant, thus, changing the recombining ion from N_2H^+ to $H^+(N_2)_2$. These competitive types of reactions have been clearly illustrated in a previous study of $HCNH^+$ and $H^+(HCN)_2$ [17,18] and more extensively for protonated and proton bound dimer forms of C_6H_6 benzene, C_5H_5N pyridine and $C_4H_4N_2$ pyrimidine [19]. To ensure that only the protonated species is recombining, studies were made of the recombination rate constant as a function of reactant gas concentration (the details of this are discussed below).

There are important experimental reasons for isotopic studies relating to the storage ring measurements. Often heteronuclear isotopic species are used since these radiatively relax whereas those, which are homonuclear do not since they have no dipole moment. This has been discussed by Guberman [20] for $^{14}N_2^+$ versus $^{14}N^{15}N^+$. Work by Kella et al. [21] has shown that even with heteronuclear N_2^+, the recombining ion is not fully relaxed. Also, $^{14}N^{15}N^+$, in its lowest vibrational state recombines 26% faster than $^{14}N_2^+$ in the same state. It needs to be established if there are similar effects for N_2H^+.

In addition, as the recombining ion gets more massive, it becomes increasingly difficult in the storage ring to distinguish neutral products which are one amu apart, i.e., differing by only one H-atom. This can be mitigated by substituting D for H, i.e., doubling the mass difference. However, it is not known how this exchange influences the recombination. The present flowing afterglow studies will address these issues.

Studies of the recombination of the various isotopic forms of N_2H^+ will also provide information on the reaction mechanisms. For all of these recombinations, the potential curves are identical since they only depend on the pure electronic Hamiltonian. The only differences are then in the spacings of the vibrational and rotational levels due to the differing masses. These masses can be expressed in term of the reduced masses, which can be determined by considering N_2H^+ as a diatomic N_2–H^+. This is reasonable since, under recombination, the N_2H^+ fragments to N_2 plus H. The reduced masses, μ, for the combinations, $^{14}N_2H^+$, $^{14}N_2D^+$, $^{15}N_2H^+$, $^{15}N_2D^+$ thus take on the values 0.966, 1.867, 0.968, and 1.875. These values can be compared with, 0.875, 1.556, 0.882, and 1.579, deduced from $1/\mu = 1/m_1 + 1/m_2 + 1/m_3$. Then the vibrational energy levels are spaced by $h/2\pi(k/\mu)^{1/2}$, where k is the force constant which is independent of isotopic form.

Note that there are two basic mechanisms for dissociative electron–ion recombination, the direct and the indirect processes. In the direct process, the neutralized N_2H^+ ion accesses a repulsive potential curve to the products $N_2 + H$. In the indirect process, the neutralized ion undergoes a radiationless transition to a highly excited Rydberg state which then undergoes a transfer to the same repulsive curve as for the direct process. For the direct mechanism, a variation in μ will change the point at which the N_2H^+ potential curve and the repulsive $N_2 + H$ curve cross relative to the vibrational levels. For the indirect mechanism, the vibrational levels in both the recombining ion and the Rydberg states will change relative to the repulsive curve. However, since the forms of the potential curves are not readily known, it cannot be predicted where there are resonances between the Rydberg state and the position of the crossing to the repulsive state and between the vibrational levels in the bound ion state and the Rydberg state.

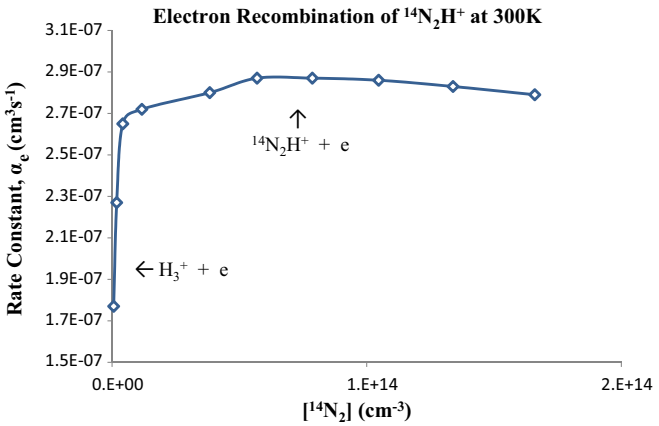

Fig. 1. Variation of reaction rate constant, α_e, with N_2 concentration, $[N_2]$, for the electron recombination of $^{14}N_2H^+$ at 300 K.

2. Experimental

The operation of the flowing afterglow for studying dissociative electron–ion recombination has been discussed in detail previously [22,23] and thus only the aspects relevant to the present study will be discussed here. Upstream in the flow tube, a plasma is created in He (pressure ~1.5 Torr) in a microwave discharge. This plasma is carried along the flow tube to a downstream mass spectrometer by the He carrier gas. The plasma ionization density is determined as a function of position along the flow with an axially moveable Langmuir probe. The N_2H^+ recombining ions of interest are created by adding Ar, H_2 and the N_2 reactant gas sequentially to the flow generating the reaction sequence:

$$He^+ + 2He \rightarrow He_2^+ + He \quad (6)$$

$$He_2^+, He^m + Ar \rightarrow Ar^+ + 2He/He + e \quad (7)$$

$$Ar^+ + H_2 \rightarrow ArH^+/H_3^+ \quad (8)$$

$$H_3^+ + N_2 \rightarrow N_2H^+ + H_2 \quad (9)$$

where the nitrogen is either $^{14}N_2$ or $^{15}N_2$ and the hydrogen is either H_2 or D_2 (He^m is the helium metastable) individually producing the recombining ions, $^{14}N_2H^+$, $^{14}N_2D^+$, $^{15}N_2H^+$, and $^{15}N_2D^+$. The recombination rate constant, α_e, is determined from the slope of a plot of 1/[e] versus axial position z along the flow (Eq. (10)),

$$[e]^{-1}_z - [e]^{-1}_0 = -\alpha_e z/v_p \quad (10)$$

where v_p is the He plasma flow velocity and z is the axial position. If only one ion species is present in the flow, this plot will be linear until ambipolar diffusion becomes the dominant ionization loss process at low ionization density. In addition, if the ion type is not changing, α_e will be independent of the concentration of the N_2 reactant gas. A plot of this form is shown in Fig. 1 for $^{14}N_2H^+$ recombination.

The variation of α_e at low $[N_2]$ is the conversion of a slowly recombining H_3^+ plasma [24] into an N_2H^+ plasma (reaction (9)). Above this region, α_e is independent of $[N_2]$ i.e., at higher flows, it shows that only one recombining ion is present. Such detailed plots could not be generated for $^{15}N_2H^+$ because of the expense. However, all studies were made under conditions where α_e was constant and are, thus, for a single recombining ion N_2H^+. To investigate the conditions where the ion type could be changing with increasing $[N_2]$ flow, for example where association could occur and $H^+(N_2)_2$ be created, the temperature of the flow tube was

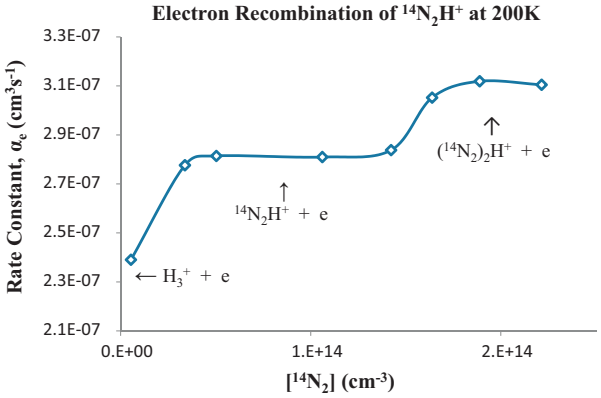

Fig. 2. Variation of reaction rate constant, α_e, with N_2 concentration, $[N_2]$, for the electron recombination of $^{14}N_2H^+/H^+(^{14}N_2)_2$ at 200 K.

lowered to 200 K since it is known that three body association is competitive since (see Eq. (5)) rate constants increase rapidly with decreasing temperature [19]. A plot of this recombination is shown in Fig. 2 and has many similarities to Fig. 1 except that at the higher $[N_2]$ there is a second increase in α_e correlated with the generation of the proton bound dimer. $H^+(N_2)_2$. This situation can be expressed by the equations:

$$\underset{e\downarrow}{H_3^+} + N_2 \rightleftharpoons N_2H^+ + H_2 \quad (11)$$

$$\underset{e\downarrow}{N_2H^+} + N_2 + He \rightleftharpoons \underset{e\downarrow}{H^+(N_2)_2} + He \quad (12)$$

Rate constants obtained in this way for $^{14}N_2H^+$, $^{14}N_2D^+$, $^{15}N_2H^+$, and $^{15}N_2D^+$ are listed in Table 1 for 300 and 500 K. Absolute errors in the rate constants are ±15%, and importantly, the relative errors are ±5%. Relative errors were evaluated by studying a series of identical reactions over an extended period of time using the same setup. Absolute errors include the systematic error associated with the experimental technique.

3. Results and discussion

Table 1 shows a comparison between the rate constants for the various isotopic forms of N_2H^+ at both 300 and 500 K. For $^{14}N_2H^+$ and $^{14}N_2D^+$, there is excellent agreement with the earlier studies [25], included in Table 1. Ratios of the rate constants are given in Table 2. A great deal can be gleaned from these tables. Firstly, the values of α_e at 500 K are consistently larger than those at 300 K. At both 300 and 500 K, the rate constants of ions containing H are larger than those containing D for both ^{14}N and ^{15}N. $\alpha_e(^{14/15}N_2D^+)/\alpha_e(^{14/15}N_2H^+) \sim 0.765/0.857$ at 300 K and 0.820/0.795 at 500 K respectively. Those containing ^{14}N are larger than those containing ^{15}N for both H and D but only at 300 K. At 500 K, the values are independent of whether the ion contains ^{14}N or ^{15}N. This is a very significant finding in that isotopic substitution of nitrogen in N_2H^+ affects the temperature dependence of the rate constant of the ion, thus, substantially influencing the recombination of the ion. Based on these observations, the rate constants for $^{14}N^{15}NH^+$ and $^{15}N^{14}NH^+$, will be greater with increasing temperature. At both 300 and 500 K, those containing H are larger than those containing D. At 500 K, the values for all combinations of ^{14}N and ^{15}N are expected to be the same. At 300 K, the values for the values for $^{14}N^{15}NH^+$ are expected to be in between those for $^{14}N_2H^+$ and $^{15}N_2H^+$ for both H and D. However, it is not easy to come to any detailed conclusions when comparing homo and hetero species. Nontheless, it is clear that the rate constants for H containing species cannot be assumed to be equal to those for their D counterparts.

Table 1
Dissociative recombination, α_e, of isotopic forms of N_2H^+ (containing H/D and $^{14}N_2/^{15}N_2$) at 300 and 500 K. Units are 10^{-7} cm^3 s^{-1}. Previous values in the literature [25] are given for $^{14}N_2H^+$ and $^{14}N_2D^+$ in parenthesis.

	$^{14}N_2H^+$	$^{14}N_2D^+$	$^{15}N_2H^+$	$^{15}N_2D^+$
200 K	2.81	–	–	–
300 K	2.77 (2.80) [25]	2.12 (2.15) [25]	2.31	1.98
500 K	2.84	2.33	2.93	2.33

Table 2
Ratios of recombination rate constants for N_2H^+ in the isotopic combinations indicated.

	$^{14}N_2D^+/^{14}N_2H^+$	$^{15}N_2D^+/^{15}N_2H^+$	$^{15}N_2H^+/^{14}N_2H^+$	$^{15}N_2D^+/^{14}N_2D^+$
300 K	0.769	0.854	0.833	0.940
500 K	0.826	0.800	1.03	1.00

Table 3
Room temperature (300 K) recombination rate constants, α_e, for the series of ions indicated, as obtained from the literature. Comparisons are given for fully hydrogenated and fully deuterated species determined using flowing afterglows (FA) and storage rings (SR). Also shown are the ratios of the rate constants $\alpha_e(D)/\alpha_e(H)$.

Molecule	α_{eH}(300 K)	α_{eD}(300 K)	α_{eD}(300 K)/α_{eH}(300 K)
N_2D^+	2.8(−7)FA [25]	2.15(−7)FA [25]	0.769
	2.77(−7)FA	2.12(−7)FA	
	Present	Present	0.765
DCO^+	2.0(−7)FA [26]	1.7(−7)FA [26]	0.85
	1.9(−7)FA [27]		
			0.769FA [25]
D_3O^+	4.3(−7)SR [28]	4.5(−7)SR [28]	1.05
	7.6(−7)SR [29]	3.5(−7)SR [29]	
	8.0(−7)FA [27]		
			0.46
D_3S^+	3.7(−7)FA [30]	2.8(−7)SR [33]	0.757
	5.2(−7)FA [31]		
	5(−7)FA [32]		
			0.539
			0.560
N_2OD^+	4.2(−7)FA [30]	1.4(−6)SR [34]	3.33
	4.5(−7)FA [27]		
DCO_2^+	3.4(−7)FA [30]	1.4(−6)SR [34]	4.11
	4.6(−7)FA [27]		4.00
			3.04
$D^+(D_2O)_2$	2.5(−6)FA [35]	1.59(−6)SR [36]	0.636
CD_3CND^+	3.3(−7)FA [37]	8.13(−7)SR [38]	2.46
$C_3D_7^+$	19(−7)SR [39]	2.3(−7)SR [41]	0.121
	8.3(−7)FA [40]		
$C_4D_9^+$	8.3(−7)FA [40]	5.8(−7)SR [41]	0.699
$C_2D_5^+$	9.0(−7)FA [27]	2.8(−7)SR [42]	0.311
	6.0(−7)FA [40]		
			0.467

4. Conclusions

These studies have shown that there are significant differences between the values of rate constants for the hydrogenated and deuterated counterparts of N_2H^+. Thus, the values deduced from storage ring studies of the deuterated species cannot be applied directly to situations involving hydrogenated species. However, note that the effects for ^{14}N and ^{15}N substitution are seen to be smaller than for H and D. It can be seen from Tables 1 and 2 that, with decreasing temperature, the ratio $^{14}N_2H^+/^{14}N_2D^+$ increases and the α_e becomes smaller. Thus, the overall concentrations of both $^{14}N_2H^+$ and $^{14}N_2D^+$ will increase, that of $^{14}N_2D^+$ increasing more rapidly. This is consistent with the studies of Fontani et al. where $^{14}N_2D^+/^{14}N_2H^+$ was measured at the much lower temperature of the interstellar clouds [11]. Fontani reported an average value of ~0.015 for the $^{14}N_2D^+/^{14}N_2H^+$ ratio in the high-mass protostellar cores observed, around 3 orders of magnitude larger than the interstellar D/H ratio.

It is interesting to compare the effects of deuteration on the electron–ion recombination rate constants from the literature. These data are compiled in Table 3. These results may not be directly comparable to the present study because several values were evaluated in different apparatuses at different times.

The ratios quoted, which vary from ∼0.3 to ∼3, are for various combinations of FA and SR, both FA and both SR (both with the same and different apparatuses). Even when H and D measurements are made using the same apparatus, there are significant differences. For example, for D_3O^+, the ratio is 1.05 from ASTRID [28] and 0.46 from CRYRING [29]. For N_2D^+, two values in the same FA are 0.765 and 0.769. However, for DCO^+, good agreement (0.85 and 0.769) is still obtained with different FA's. There is much less experimental data available for the ^{14}N–^{15}N isotopic comparison, and a similar table cannot be tabulated. Thus, the overall conclusion is that a little more faith can be put in the FA values than from those in the SR, but there is a great deal of work that needs to be done. Also, many more calculations are required to establish the effects of isotopic composition.

Acknowledgements

Funding by NASA under grant # NNX10AC76G is gratefully acknowledged.

References

[1] E. Roueff, M. Gerin, Space Sci. Rev. 106 (2003) 61–72.
[2] R. Terzieva, E. Herbst, Mon. Not. R. Astron. Soc. 317 (2000) 563–568.
[3] S.D. Rodgers, S.B. Charnley, Mon. Not. R. Astron. Soc. 385 (2008) L48–52.
[4] M. Gerin, N. Marcelino, N. Biver, E. Roueff, L.H. Coudert, M. Elkeurti, D.C. Lis, D. Bockelee, Astron. Astrophys. 489 (2009) L9–12.
[5] D.C. Lis, A. Wootten, M. Gerin, E. Roueff, Asrtophys. J. Lett. 710 (2010) L49–52.
[6] L. Bizzocchi, P. Caselli, L. Dore, Astron. Astrophys. (2010).
[7] A.A. Stark, Astrophys. J. 245 (1981) 99–104.
[8] D. Bockelee-Morvan, N. Biver, E. Jehin, A.L. Cochran, H. Wiesemeyer, J. Manfroid, D. Hutsemekers, C. Arpigny, J. Boissier, W. Chockran, P. Colom, J. Corvisier, N. Milutinovic, R. Moreno, J.X. Prochaska, I. Ramirez, R. Schulz, J.-M. Zucconi, Astrophys. J. Lett. 679 (2008) L49–52.
[9] H. Busemann, A.F. Young, M. Conel, O.D. Alexander, P. Hoppe, S. Mukhopadhyay, L.R. Nittler, Science 312 (2006) 727–730.
[10] A. Crapsi, P. Caselli, C.M. Walmsley, P.C. Myers, M. Tafalla, C.W. Lee, T.L. Bourke, Astrophys. J 619 (2005) 1–35.
[11] F. Fontani, P. Caselli, A. Crapsi, R. Cesaroni, S. Molinari, L. Testi, J. Brand, Los Alamos National Laboratory, Preprint Archive, Astron. Astrophys. (2008) 1–27, arX iv:astro-ph/0608702.
[12] N.G. Adams, D. Smith, Astrophys. J. 247 (1981) L123–L125.
[13] C.D. Molek, V. Poterya, N.G. Adams, J.L. McLain, Int. J. Mass Spectrom. 285 (2009) 1–11.
[14] W. Geppert, R. Thomas, J. Semaniak, A. Ehlerding, T.J. Millar, F. Osterdahl, M. af Ugglas, N. Djuric, A. Paal, M. Larsson, Astrophys. J. 609 (2004) 459–464.
[15] C.D. Molek, J.L. McLain, V. Poterya, N.G. Adams, J. Phys. Chem. A 111 (2007) 6760–6765.
[16] W.D. Geppert, M. Larsson, Mol. Phys. 106 (2008) 2199–2226.
[17] J.L. McLain, C.D. Molek, D. Osbourne, N.G. Adams, Int. J. Mass Spectrom. 282 (2009) 85–90.
[18] J. McLain, N.G. Adams, Planet. Space Sci. 57 (2009) 1642–1647.
[19] N.G. Adams, L.D. Mathews, D.S. Osborne, Faraday Discuss. 147 (2010), 1-323-335.
[20] S.L. Guberman, in: S.L. Guberman (Ed.), Dissociative Recombination of Molecular Ions with Electrons, Kluwer, New York, 2003, pp. 187–196.
[21] D. Kella, P.J. Johnson, H.B. Pedersen, L. Vejby-Cristensen, L.H. Andersen, Phys. Rev. Lett. 77 (1996) 2432–2435.
[22] E. Alge, N.G. Adams, D. Smith, J. Phys. B 16 (1983) 1433–1444.
[23] D. Smith, N.G. Adams, in: F. Brouillard, J.W. McGowan (Eds.), Physics of Ion–Ion and Ion–Electron Collisions, Plenum Press, New York, 1983, pp. 501–531.
[24] J. Glosik, R. Plasil, I. Korolov, O. Novotny, T. Kotrik, J. Phys. Conf. Ser. 192 (2009) 012005.
[25] V. Poterya, J.L. McLain, N.G. Adams, L.M. Babcock, J. Phys. Chem. A 109 (2005) 7181–7186.
[26] I. Korolov, R. Plasil, T. Kotrik, P. Dohnal, J. Glosik, Int. J. Mass Spectrom. 280 (2009) 144–148.
[27] T. Gougousi, M.F. Golde, R. Johnsen, Chem. Phys. Lett. 265 (1997) 399–403.
[28] M.J. Jensen, R.C. Bilodeau, C.P. Safvan, K. Seiersen, L.H. Andersen, H.B. Pedersen, O. Heber, Astrophys. J. 543 (2000) 764–774.
[29] A. Neau, A.A. Khalili, S. Rosen, A. Le Padellec, A.M. Derkatch, W.S.L. Vikor, J. Semaniak, R. Thomas, M.B. Nagard, K. Anderson, H. Danared, M. af Ugglas, J. Chem. Phys. 113 (2000) 1762–1770.
[30] N.G. Adams, D. Smith, Chem. Phys. Lett. 144 (1988) 11–14.
[31] H. Abouelaziz, J.L. Queffelec, C. Rebrion, B.R. Rowe, J.C. Gomet, A. Canosa, Chem. Phys. Lett. 194 (1992) 263–267.
[32] B.R. Rowe, A. Canosa, V. Le Page, Int. J. Mass Spectrom. Ion Proc. 149/150 (1995) 573–596.
[33] M. Kaminska, E. Vigren, V. Zhaunerchyk, W.D. Geppert, H. Roberts, C. Walsh, T.J. Millar, M. Danielson, M. Hamberg, R.D. Thomas, M. Larsson, M. af Ugglas, J. Semaniak, Astrophys. J. 681 (2008) 1717–1724.
[34] W. Geppert, R. Thomas, F. Hellberg, A. Ehlerding, F. Osterdahl, M.a. Ugglas, M. Larsson, Phys. Chem. Chem. Phys. 6 (2004) 3415–3419.
[35] C.-M. Huang, M. Whitaker, M.A. Biondi, R. Johnsen, Phys. Rev. A 18 (1978) 64–67.
[36] M.B. Nagard, J.B.C. Pettersson, A.M. Derkatch, A. Al Khalili, A. Neau, S. Rosen, M. Larsson, J. Semaniak, H. Danared, A. Kallberg, F. Osterdahl, M. af Ugglas, J. Chem. Phys. 117 (2002) 5264–5270.
[37] M. Geoghegan, N.G. Adams, D. Smith, J. Phys. B 24 (1991) 2589–2599.
[38] E. Vigren, M. Kaminska, M. Hamberg, V. Zhaunerchyk, R.D. Thomas, M. Danielsson, J. Semaniak, P.U. Andersson, M. Larsson, W.D. Geppert, Phys. Chem. Chem. Phys. 10 (2008) 4014–4019.
[39] A. Ehlerding, S. Arnold, A.A. Viggiano, S. Kalhori, J. Semaniak, A. Derkatch, S. Rosén, M. af Ugglas, M. Larsson, J. Phys. Chem. A 107 (2003) 2179–2189.
[40] L. Lehfaoui, C. Rebrion-Rowe, S. Laube, B.A. Mitchell, B.R. Rowe, J. Chem. Phys. 106 (1997) 5406–5412.
[41] M. Larsson, A. Ehlerding, W. Geppert, F. Hellberg, S. Kalhori, F. Osterdahl, G. Angelova, J. Semaniak, O. Novotny, S.T. Arnold, A.A. Viggiano, J. Chem. Phys. 122 (2005) 156101–156103.
[42] W. Geppert, A. Ehlerding, F. Hellberg, S. Kalhori, R. Thomas, O. Novotny, S.T. Arnold, T.M. Miller, A.A. Viggiano, M. Larsson, Phys. Rev. Lett. 93 (2004) 153201–153204.